KSÜ Mühendislik Bilimleri Dergisi, 29(3), 2026
Araştırma Makalesi

KSU J Eng Sci, 29(3), 2026
Research Article

Kahramanmaras Sutcu Imam University
Journal of Engineering Sciences

Geliş Tarihi : 03.10.2025
Kabul Tarihi : 12.01.2026

Received Date : 03.10.2025
Accepted Date : 12.01.2026

ULTRA THIN METAMATERIAL ABSORBER FOR 5G APPLICATIONS

5G UYGULAMALARI İÇİN ULTRA İNCE METAMALZEME SOĞURUCU

Emin ÜNAL [1] (ORCID: 0000-0002-4088-8353)
Mahad Ali IBRAHIM [1] (ORCID: 0000-0001-5581-9118)
Fatih Özkan ALKURT [2]* (ORCID: 0000-0002-9940-0658)
Maide ERDOĞAN ALKURT [2] (ORCID: 0000-0003-1858-510X)

[1] Necmettin Erbakan University, Faculty of Engineering, Department of Electrical and Electronics Engineering, Konya, Türkiye
[2] Iskenderun Technical University, Faculty of Engineering and Natural Sciences, Department of Electrical-Electronics Engineering, Hatay, Türkiye
*Sorumlu Yazar / Corresponding Author: Fatih Özkan ALKURT, fozkan.alkurt@iste.edu.tr

ABSTRACT

This work is based on an ultra-thin, and polarization-insensitive metamaterial absorber specifically designed for Ku/Ka-band applications. For this purpose, metamaterial-based absorber structures operating at microwave frequencies have been designed. The metamaterial absorber structure designed in this study is completely novel. Numerical and simulation studies of the signal absorber structures operating at microwave and optical frequencies have been performed using a finite integration technique (FIT) based simulation program. The proposed absorbers have been found to have nearly perfect absorption over 90% for TE and TM polarizations, covering the entire Ku/Ka band under normal incidence. In order to better understand the absorption mechanism, the electric and magnetic field distributions on the resonator structure and also the surface current distributions have been investigated. Simulation studies have been conducted in the Ku/Ka bands. Furthermore, to verify the accuracy of the simulations, the fabrication and measurement of the designed Ku-band structure have also been performed. The Ku-band signal absorber structures have been fabricated using the LPKF ProtoMat E33, and experimental measurements have been made using a horn antenna and a PNA-L N5234A Microwave Network Analyzer. A double-sided copper-clad RT5870 substrate has been used in the fabrication. Because the back side of the fabricated structure is completely copper-clad, only the reflection parameter (S11) was measured. Numerical and experimental results have been compared, and good agreement has been found between the results. This study is important for electromagnetic shielding, cloaking technologies and improving antenna performance.

Keywords: Metamaterial, absorber, microwaves

ÖZET

Bu çalışma, Ku/Ka-bant uygulamaları için özel olarak tasarlanmış ultra ince ve polarizasyona duyarsız bir metamalzeme soğurucuya dayanmaktadır ve bu amaçla, mikrodalga frekansında çalışan metamalzeme tabanlı soğurucu yapılar tasarlanmıştır. Bu çalışmada tasarlanan metamalzeme soğurucu yapı tamamen özgündür. Mikrodalga ve optik frekanslarda çalışan sinyal soğurucu yapıların sayısal ve simülasyon çalışmaları, sonlu entegrasyon tekniği (FIT) tabanlı bir simülasyon programı kullanılarak gerçekleştirilmiştir. Önerilen soğurucuların TE ve TM polarizasyon için normal gelişte tüm Ku/Ka bandını kapsayan %90'ın üzerinde neredeyse mükemmel bir soğuruculuğa sahip olduğu görülmüştür. Soğurma mekanizmasının daha iyi anlaşılabilmesi için rezönatör yapı üzerindeki elektrik ve manyetik alan dağılımları ve ayrıca yüzey akım dağılımları da incelenmiştir. Simülasyon çalışmaları Ku/Ka bantlarında gerçekleştirilmiştir. Diğer taraftan, simülasyon çalışmalarının doğruluğunu test edebilmek için Ku bandında tasarlanan yapının üretim ve ölçümü de yapılmıştır. Ku bandında çalışan sinyal soğurucu yapıları LPKF ProtoMat E33 kullanılarak üretilmiş ve deneysel ölçümler, horn anten ve PNA-L N5234A Mikrodalga Ağ Analizörü kullanılarak yapılmıştır. Üretimde çift tarafı bakır kaplı RT5870 alt tabaka kullanılmıştır. Üretilen yapının arka tarafı tamamen bakırla kaplı olduğu için sadece yansıma parametresi (S11) ölçülmüştür. Sayısal ve deneysel sonuçlar birbirleriyle karşılaştırılmış ve sonuçlar arasında iyi bir uyumun olduğu görülmüştür. Bu çalışma, elektromanyetik kalkanlama, gizleme ve anten performansının iyileştirilmesi açısından önem taşımaktadır.

Anahtar Kelimeler: Metamalzeme, absorber, mikrodalgalar

INTRODUCTION

Today, the development of communication technologies is rapidly increasing. In parallel with the advancements in wireless communication technologies, the need for efficient electromagnetic absorbers that can cope with challenges such as energy harvesting, signal interference, and radar cross-section reduction, especially in the Ku/Ka-band frequency range (12-18 GHz and 26.5-40 GHz), is increasing. In this field, metamaterials have emerged as an innovative solution due to their unique ability to manipulate electromagnetic waves (EM) at subwavelength scales (Pendry et al., 2006). These artificially designed and produced materials have exhibited properties not found in nature, such as negative refractive index and high anisotropy, enabling the design of ultrathin, lightweight, and high-performance absorbers.

Metamaterial absorbers have attracted much attention in the scientific community due to their almost perfect absorption ability in a certain frequency range, which has made them potential for applications in satellite communications, 5G networks, and cloaking technologies (Singh et al., 2021). However, despite their wide application areas, the common metamaterial absorbers found in the literature have drawbacks such as narrow bandwidth, bulky structure, and sensitivity to the polarization of incident waves, which limit their practical use. This study aims to overcome these aforementioned drawbacks by proposing a broad-band, ultrathin, and polarization-insensitive metamaterial absorber specifically designed for Ku/Ka-band applications. Ku/Ka-band, widely used in satellite communications and emerging 5G technologies, requires absorbers that can operate efficiently across a wide frequency range while maintaining a compact and lightweight profile. Current designs often struggle to achieve this balance, as increased bandwidth often requires coarser structures or complex geometries that are impractical for many applications. Furthermore, because the polarization properties of electromagnetic waves can vary in real-world environments, polarization sensitivity remains a significant challenge. The proposed absorber aims to overcome these challenges by offering high absorption efficiency, wide frequency range, and polarization insensitivity with its ultrathin structure. Metamaterials can be defined as artificial materials engineered to achieve superior, unnatural properties by tailoring their materials' effective electric and magnetic response. These materials typically consist of periodic patterns arranged in periodic cells whose unit cell size is much smaller than the operating wavelength. The properties of metamaterials can be precisely tuned to manipulate incoming electromagnetic waves; that is, they can control, direct, redirect, focus, absorb, and reflect them in various ways. This precise control of electromagnetic waves has led to the application of metamaterials in fields such as electromagnetic cloaking, perfect absorbers, energy harvesting, and diffraction-beyond-the-limit imaging.

Metamaterials are also known as negative refractive index materials and left-handed materials. One of the most well-known properties of metamaterials is the ability to achieve a negative refractive index by exploiting electric and magnetic resonance (dielectric constant, $\varepsilon < 0$, and magnetic permeability, $\mu < 0$, respectively) (Smith et al., 2004). This discovery has led to new types of applications such as superlenses, near-diffraction imaging, stealth, and cloaking. Metamaterials can also find applications in improving solar energy efficiency (Kıymaz and Oğuz, 2024; Akkoyunlu et al., 2024) and antenna performance (Ateş et al., 2019). High-impedance surfaces, consisting of metal and dielectric thin film layers whose geometric shapes and dimensions are precisely controlled to exhibit desired properties such as phase shift and frequency-selective responses, are known as another type of metamaterials. When the effective surface impedance of a high surface impedance matches the impedance of free space, excellent absorption can be achieved within a specific band gap (Engheta, 2002). These surfaces are commonly referred to as perfect metamaterial absorbers and can be used in a wide electromagnetic band from microwaves to the optical spectrum.

Perfect absorbers have long been investigated for various applications, including wireless communications, thermal

emitters, sensors, photodetectors, and photovoltaic structures. The design of such absorbers is based on the principle of minimizing reflected and transmitted power, and in most cases, the incident power is converted to heat, which can be used in another form of energy harvesting application. Unlike other metamaterial devices, which generally require losses to be avoided, metamaterial absorbers primarily exploit losses arising from the finite resistivity of the metal or from dielectric loss in the system (Watts et al., 2012). Metamaterial absorbers, properly designed for their operating frequency range, can find applications across virtually the entire electromagnetic spectrum, including radio frequencies (RF), microwaves, the THz region, infrared, and the visible spectrum. While many metamaterial absorbers are characterized as nearly perfect absorbers, there are important parameters to consider when designing application-specific metamaterial absorbers, such as bandwidth, angle of incidence, and polarization sensitivity. Depending on the design specifications, metamaterial absorbers can be applied to a wide range of applications, including energy harvesting, solar cells, sensing, communications, radar, shielding, and more.

In recent years, studies on metamaterial absorbers and their applications have continued with a wide variety of objectives and design features. A significant portion of these studies have focused on energy harvesting applications of metamaterial absorbers (Ünal et al., 2015; Nowak, 2021). Some of the energy harvesting studies have focused on the more specific area of solar energy harvesting (Bağmancı et al., 2017; Liu et al., 2021). In general, studies on metamaterial absorber applications cover all bands of the electromagnetic spectrum from radio waves to visible light. Some of these studies are studies on Ku/K/Ka/5G (mm-Wave) band applications (Khanna and Awasthi, 2020; Bilal et al., 2021; Chung et al., 2022; Hakim et al., 2023; Zhu et al., 2025). Various studies have also been carried out on polarization-insensitive oblique incidence angle stabilization and metamaterial absorber structures based on ultrathin nano-rings operating in the higher frequency band, Terahertz (THz) (Zhong et al., 2020; Nickpay et al., 2021; Hanif et al., 2023). Additionally, various academic studies have been conducted on broad-band metamaterial absorber structures using truncated nanocones with colloidal lithography (Guo et al., 2021), ultrathin tunable metamaterial absorber based on magnetic nanomaterial (Ning et al., 2022), and broad-band, ultrathin, polarization-insensitive metamaterial absorber structures (Saadeldin et al., 2023a; Saadeldin et al., 2023b; Uddin et al., 2025).

In summary, this study introduces a novel, ultra thin, and polarization insensitive metamaterial absorber for Ku/Ka bands. The absorber shows nearly 90% absorption for both TE and TM polarizations, under simulations and experimental measurements. Field and surface current analyses reveal the absorption mechanisms, and the close match between simulations and measurements confirms the design validity.The proposed structure has a great potential for applications in electromagnetic shielding, stealth, and antenna performance enhancement.

MATERIALS AND METHODS

Metamaterials have a wide range of applications, including optical filters, medical devices, aerospace applications, sensor detection, absorbers, energy harvesting, superlenses, cloaking, radomes, antennas, etc. One of the most important applications where these structures are used is known as perfect absorption. To achieve perfect absorption, the transmittance and reflectance must be reduced to zero simultaneously, so that all incident electromagnetic waves are absorbed by the material. Since they are subwavelength structures relative to the incident wavelength, metamaterial absorbers behave like an effective material, despite being composed of different layers. Therefore, the properties of metamaterial absorbers are determined by effective parameters called electric permittivity and magnetic permeability. In particular, with the help of these parameters, the effective impedance of the absorber can be adjusted to be the same as the impedance of free space (Landy et al., 2008).

To better understand and verify the working principle of metamaterial signal absorbing structures, theoretical studies need to be confirmed by numerical and experimental studies (Saadeldin et al., 2023b; Uddin et al., 2025). The frequency-dependent absorption of a material can be defined in relation to transmittance $T(\omega)$ and reflectance $R(\omega)$ as given in Equation 1 below:

$$A(\omega) = 1 - R(\omega) - T(\omega) = 1 - S_{11}^2 - S_{21}^2 \quad (1)$$

Here, S_{11} and S_{21} represent the reflection coefficient and transmission coefficient, respectively. In metamaterial signal absorber studies, the transmission coefficient becomes zero because the back plate of the metamaterial is covered with a metal plate. Rearranging Equation 1 gives:

$$A(\omega) = 1 - R(\omega) = 1 - S_{11}^2 \quad (2)$$

To ensure impedance matching at the resonance frequency, it is desired that $A(\omega)$ be maximum and $R(\omega)$ be minimum, as given in Equation 2. To minimize reflection, the impedance of the metamaterial must match the free space impedance, which is calculated using Equation 3 below:

$$Z = \sqrt{\frac{\mu}{\varepsilon}} \quad (3)$$

Here, μ and ε are the magnetic permeability and dielectric constant of the medium and are defined as $\mu = \mu_0\mu_r$, $\varepsilon = \varepsilon_0\varepsilon_r$, respectively. On the other hand, the reflectance at normal incidence can be expressed as given in Equation 4:

$$R(\omega) = \left|\frac{Z(\omega)-Z_0}{Z(\omega)+Z_0}\right|^2 \quad (4)$$

Determining the size, shape, and geometric structure of the unit cell of the metamaterial absorber is one of the most important steps in the process of designing perfect metamaterial absorber structures. This is because the absorption properties of a metamaterial absorber depend largely on its geometric arrangement rather than on its chemical composition. The Drude model plays an important role in selecting suitable materials for metamaterial absorber design (Cai and Shalaev, 2016). The selection of the numerical simulation software to be used to design the MTM absorber unit cell is another important issue in the metamaterial absorber design process. Numerous computer software that can be used for numerical analysis are commercially available, and each software offers its own advantages and limitations in the design process of metamaterial absorbers. In this study, a Finite Integration Technique (FIT) based simulation software is used for the numerical analysis, design, and characterization of the proposed metamaterial absorber.

(a) **(b)**

Figure 1. ***(a)*** *Production Using LPKF-E33,* ***(b)*** *Measurement Setup with PNA-L Microwave Network Analyzer*

The absorber structures designed in the FIT-based microwave simulation program are analyzed using the same program. The designed cell structures are periodically fabricated using a CNC-based LPKF ProtoMat E33 device, as shown in Figure 1a. All structures have been designed and manufactured in the form of a copper plate placed on a dielectric layer, with copper used as the resonator.

To evaluate the design and performance of the proposed metamaterial absorbers, in addition to numerical analysis, measurements have been performed using the PNA-L Microwave Network Analyzer and horn antenna, as shown in Figure 1b, and the results are compared. The PNA-L Network Analyzer, with its high sensitivity and wide frequency range, is used to measure the reflection coefficient (S_{11}) and transmission coefficient (S_{21}) of the metamaterial absorber, which are critical for determining the absorption properties. The horn antenna, known for its directional radiation pattern and high gain, is used to excite the metamaterial absorber with electromagnetic waves in the desired frequency spectrum (Balanis, 2016). The signals reflected from the absorber are captured by the horn antenna and analyzed by the network analyzer to evaluate the absorption efficiency and bandwidth.

This measurement setup allows characterization of the metamaterial's ability to minimize reflection and maximize energy dissipation, key metrics for evaluating its performance. The combination of PNA-L's accuracy and the horn antenna's directional capabilities provides reliable and detailed measurements, making this method indispensable for the development and validation of advanced metamaterial absorbers.

RESULTS

The designed absorber consists of double split ring copper resonators separated by a dielectric intermediate layer and a continuous copper ground plane for the Ku/Ka-band application. The metallic layers are copper with a thickness of 0.035 mm and a frequency-independent conductivity of $\sigma = 5.96 \times 10^7$ S/m. However, for both bands, the dielectric substrate is selected as low-cost Rogers RT5870 with a thickness of $h = 0.51$ mm. The dielectric constant of the Rogers RT5870 material is $\varepsilon_r = 2.33$ and the loss tangent is $\delta = 0.0012$'dir. Optimized geometry of DSRR for Ku/Ka-band is shown in Figure 2.

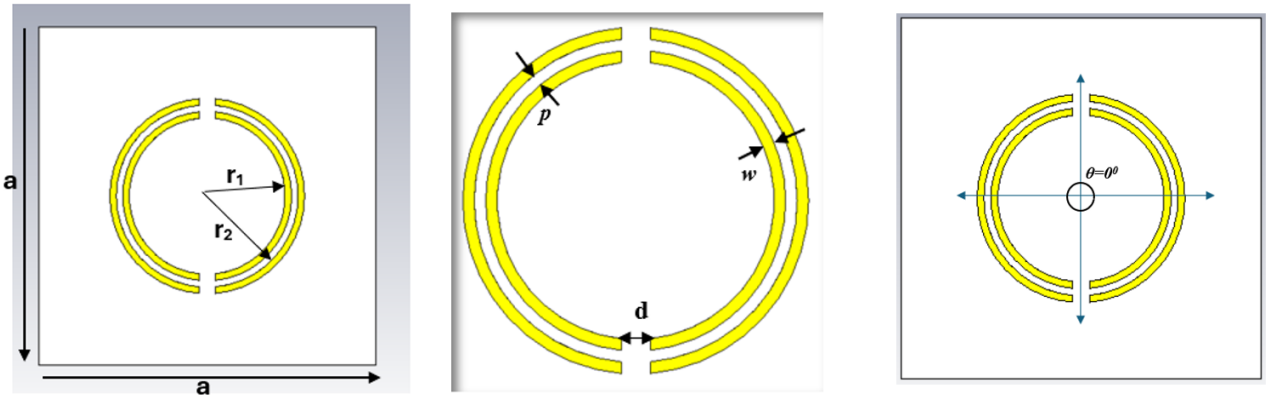

Figure 2. *Optimized Geometry of Double Split-Ring Resonators for Ku/Ka-Band*

For Ku band, the optimized dimensions of the unit cell geometry of double split ring resonators (DSRR) are: Outer radius of outer split ring $r_2 \approx 5.82$ mm. Inner radius of inner split ring $r_1 \approx 5.02$ mm, Split gap $d = 0.5$ mm (The slot in each ring controls the capacitance and greatly affects the resonant frequency). The angular orientation of DSRR within the unit cell is referenced to $\theta = 0^o$, which is especially critical for studying the polarization sensitivity. The unit cell size is 10.44 mm (length and width of the square substrate), the separation between inner and outer ring $p = 0.4$ mm (also called the gap or spacing between rings), and Ring width $w = 0.4$ mm (thickness of metallic rings).

For Ka-band, the optimized dimensions of the unit cell of DSRR are: outer radius $r_2 \approx 2.86$ mm, inner radius $r_1 \approx 2.56$ mm, split pitch $d = 0.5$ mm, separation $p = 0.1$ mm, ring width $w = 0.1$ mm, and unit cell size 5.22 mm,

angular orientation $\theta = 0^o$. The substrate is Rogers RT5870 with thickness $h = 0.51$ mm, dielectric constant $\varepsilon_r = 2.33$ and loss tangent $\delta = 0.0012$.

Scattering parameters (S-parameters) are obtained using simulation software. Reflection and transmission coefficients are obtained using the obtained S-parameters. In general, the absorption of a system can be found using the formula $A = 1 - R - T$. Since a metallic backing layer is used, transmittance is eliminated ($T = 0$), so transmittance can be ignored from the equation. Therefore, absorption spectra can be calculated directly from the reflectance using the formula $A = 1 - R$. For the Ku band, to investigate the operational stability of absorption in the azimuthal plane under different incidence angles (φ = phi), absorption results have been simulated and shown in Figure 3. The figure shows two prominent absorption peaks around the 12.8 GHz and 15 GHz frequency bands. As the φ angle increases from 0° 'to 90°, the absorption magnitude decreases significantly. At $\varphi = 0°$, the maximum absorption reaches almost 1 at the 15 GHz frequency peak, while at $\varphi = 90°$, the absorption is almost completely suppressed at all frequencies. These results show that the absorption performance is quite sensitive to the change of φ angle.

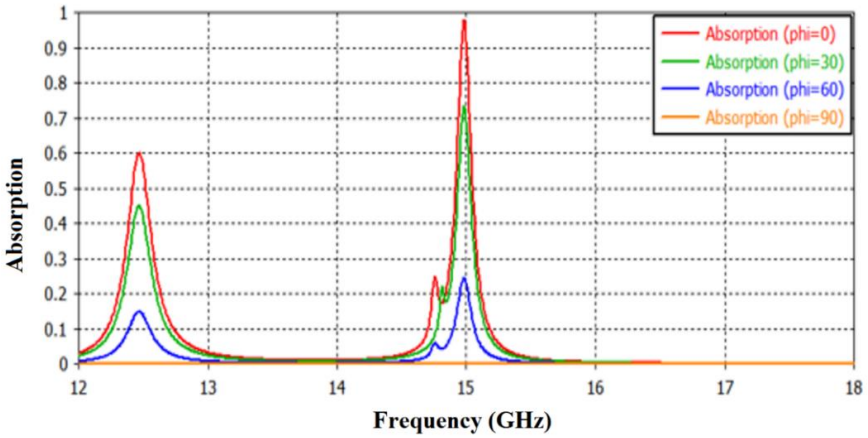

Figure 3. *Absorption Results for Different Incident Angles (φ)in Ku Band*

To investigate the operational stability of the designed structure under different azimuthal incident angles for the Ka band, the absorption results are simulated and shown in Figure 4. The figure shows distinct absorption peaks around the 32.47 GHz frequency bands. As the φ angle increases from 0° to 90°, the absorption magnitude decreases significantly. At $\varphi = 0°$, the maximum absorption reaches almost 1 at the 32.47 GHz frequency peak, while at $\varphi = 90°$, the absorption is almost completely suppressed at all frequencies. This result demonstrates that the performance of the designed structure is highly sensitive to the change of the φ angle.

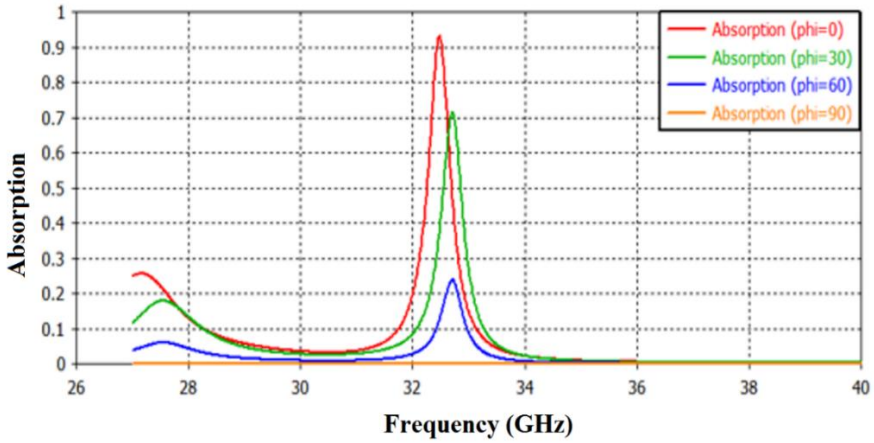

Figure 4. *Absorption Results for Different Incident Angles (φ)in Ka Band*

This study also investigates the absorption mechanism resulting from transverse electric (TE) mode propagation, with particular emphasis on the relationship between electromagnetic field distributions and surface current behavior. In TE modes, i.e., when the electric field has no longitudinal component, the study analyzes how the electric (E) and magnetic (H) field distributions, combined with their specific patterns, affect the overall absorption properties. Additionally, the surface current distributions of the proposed structure at resonant frequencies of 15 GHz and 32.47 GHz under TE mode are also investigated.

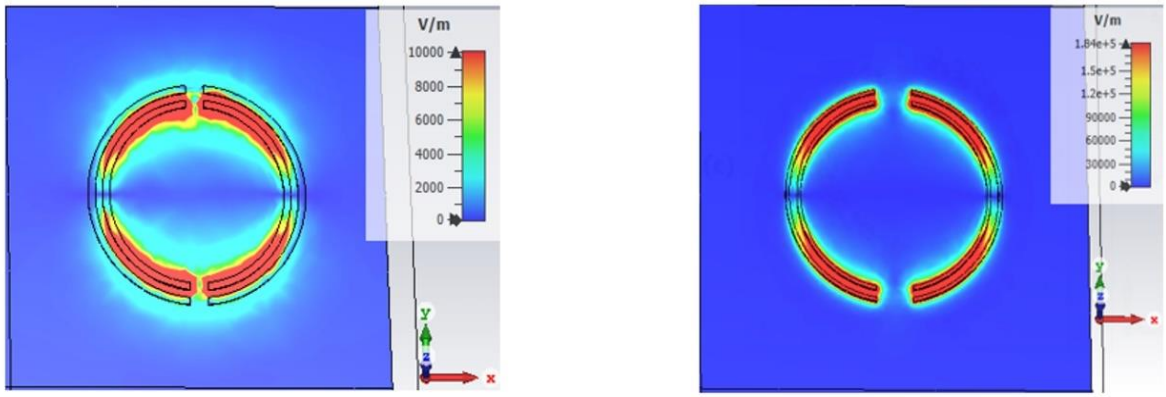

Figure 5. *Electric Field Distributions in TE Mode,* ***(a)*** *Ku-Band, 15 GHz,* ***(b)*** *Ka-Band, 32.47 GHz*

Figure 5a shows the electric field distribution for the Ku band at 15 GHz, where the maximum absorption is 98.4%. Similarly, Figure 5b shows the electric field distribution for the Ka band at 32.47 GHz, where the maximum absorption is 93%. The E-field distribution shows how the electric field is concentrated in specific regions of the unit cell at resonance. In the simulated plot, the electric field is highly concentrated across the DSRR gaps, where the electric potential difference is maximum. This concentration is indicative of strong capacitive effects resulting in electric dipole resonance. The enhanced electric response increases the effective electric permittivity (ε) of the metamaterial. Along with magnetic resonance, the electric field plays a vital role in maximizing absorption by providing effective impedance matching and energy dissipation within the lossy dielectric substrate.

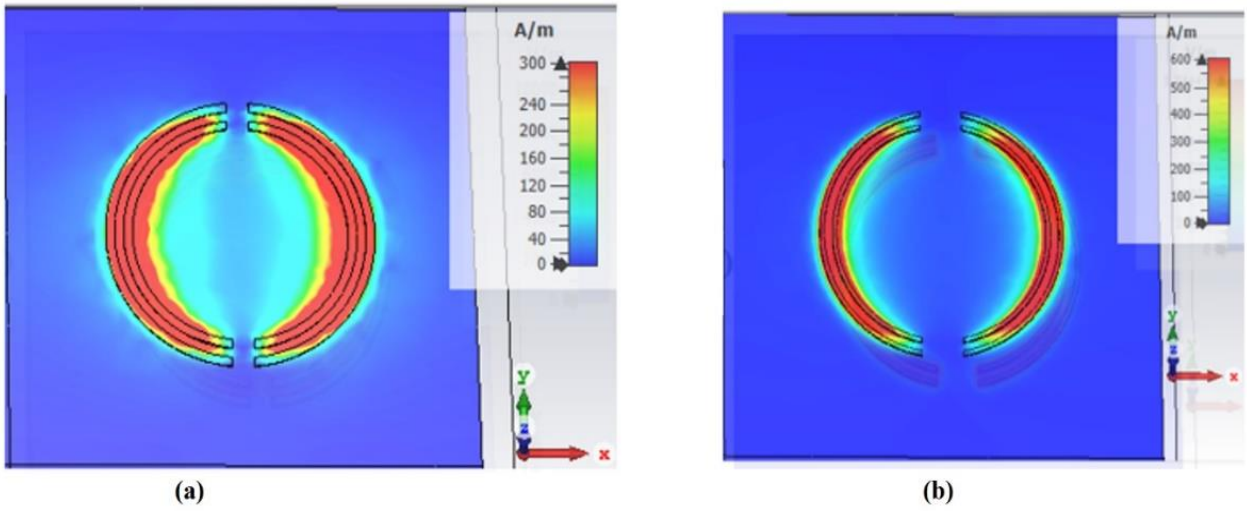

Figure 6. *Magnetic Field Distributions in TE Mode, a) Ku-Band, 15 GHz, b) Ka-Band, 32.47 GHz*

Similarly, in Figure 6a, the magnetic field distribution for the Ku band is given at 15 GHz, where the maximum absorption is 98.4%. Furthermore, for the Ka band, the magnetic field distribution at 32.47 GHz, where the maximum

absorption is 93%, is given in Figure 6b. In the simulated plot, the magnetic field is strongly localized inside the circular rings of double split ring resonators (DSRRs), particularly near the inner edges and around the ring. This strong localization indicates magnetic resonance, where the magnetic field of the incident wave induces circulating currents and leads to the storage of magnetic energy within the resonators. This resonance increases the effective magnetic permeability (μ) of the structure and is necessary to achieve impedance matching with free space. Field symmetry across the array confirms consistent resonant behavior across all unit cells.

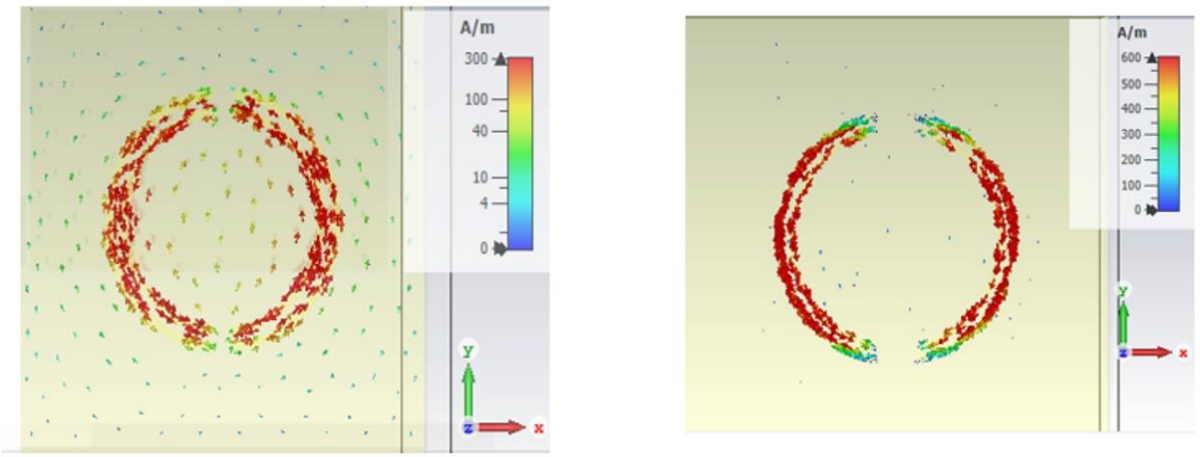

(a) (b)

Figure 7. *Surface Current Distributions in TE Mode, a) Ku-Band, 15 GHz, b) Ka-Band, 32.47 GHz*

To further explain the absorption mechanism of the ultrathin metamaterial absorber, the surface current distributions are presented in Figures 7a and b at 15 GHz for the Ku band and 32.47 GHz for the Ka band, respectively. When the electric field component of the incident electromagnetic wave interacts with the structure, it induces the motion of free electrons, generating surface currents. This motion causes surface charge oscillations along the electric field, generating a magnetic dipole moment. This dipole moment then leads to signal absorption at the resonant frequency. Similarly, the strongest surface currents are observed along the edges of split-ring resonators (DSRRs), indicating inductive loops induced by the magnetic component of the incident wave. These loops create magnetic resonances that enhance the effective magnetic response of the absorber.

The electrical response causes parallel rotating surface currents, while the magnetic response causes antiparallel rotating surface currents (Dincer et al., 2013). The induced currents in the surface cause the electric and magnetic field responses of the incident electromagnetic wave to couple, which determines the resonant frequencies for the enhancement of the localized EM field. When impedance matching conditions are met, electrical and magnetic resonance occur simultaneously, resulting in complete absorption of the incident EM wave. The absorption phenomenon occurs due to strong localized electric and magnetic field coupling between the resonator rings, that induces surface currents that dissipate the incident electromagnetic energy as heat within the substrate.

To verify the simulation results, measurements have been made in the Ku band using the setup shown in Figure 1b. The horn antenna is capable of emitting radiation at microwave frequencies between 12 and 18 GHz in the Ku band. The measured reflection coefficient (S_{11}) reached its minimum at 15.61 GHz, while the simulated reflection coefficient reached its minimum at 15 GHz; in other words, it entered resonance, and the results are shown in Figure 8. There is a frequency shift of 0.61 GHz between the results. Furthermore, a difference is observed in the S_{11} results. According to the simulation results, the S_{11} value is approximately -18 dB, while the measured S_{11} value is approximately -50 dB. It can be said that the difference between the results is mainly due to manufacturing and measurement errors, but also to diffraction scattering caused by the limited number of unit cells in the structure used in the measurement.

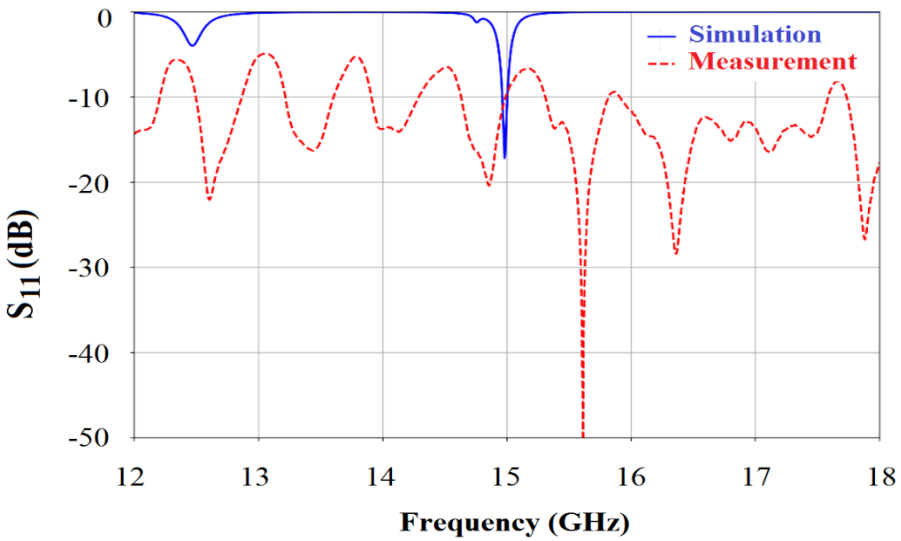

Figure 8. *Simulated and Measured S_{11} Values*

DISCUSSION AND CONCLUSIONS

This work is based on the design, simulation, and experimental investigation of a double split ring resonator (DSRR) unit cell designed as a metamaterial perfect absorber for satellite communications in the Ku-band frequency range. Simulation studies have been performed using a FIT-based simulation program. The selection of a cost-effective Rogers RT5870 substrate with double-sided copper coating resulted in a good impedance match with free space, as demonstrated by the reduction of the simulated S_{11} (Ku/Ka bands) reflection coefficient to -17.42 dB and -12 dB, corresponding to an absorption efficiency of 98.4% and 93%, respectively. The design's narrow bandwidth of 200 MHz and 90 MHz, noted between 14.9 GHz and 15.1 GHz at -10 dB, effectively overlaps with standard 36-72 MHz Ku-band channel allocations, validating its applicability for electromagnetic interference mitigation and cloaking technology applications.

Additionally, the dependence of the absorber on the incidence angle has been investigated and found to exhibit high stability at various incidence angles. Studies investigating the sensitivity to incidence angles between 0° and 90° demonstrated directional sensitivity, revealing the highest absorption at 0° and a significant decrease at 90°. Furthermore, analysis of the surface current and electromagnetic field distributions highlights the roles of magnetic flux coupling and electric dipole resonance in achieving high absorption levels, providing perspectives on the underlying physical mechanisms. The results confirmed the absorption mechanism under the TE mode, with the DSRR exhibiting strong resonance at 15 GHz and 32.47 GHz.

Experimental verification measurements performed on a 10 × 10 DSRR prototype fabricated using LPKF ProtoMat E33 using a horn antenna and a vector network analyzer are found to be in good agreement with the simulation results, thus validating the simulation results. The S_{11} minimum measured at 15.61 GHz, although slightly deviating from the simulated range of approximately 15 GHz, achieved an absorption ratio of 99.9%, slightly exceeding the simulated ratio of 98.4%. According to these results, the high absorption efficiency, narrow bandwidth, and polarization insensitivity of the proposed MA make it a suitable candidate for reducing electromagnetic interference and improving signal security. This work is important for the development of advanced electromagnetic shielding, cloaking technologies, and antenna system integration (Ibrahim, 2025). The proposed metamaterial absorber offers high functionality that is suitable for a wide range of applications. Specifically, it can be employed in electromagnetic shielding to suppress unwanted reflections, in stealth and cloaking technologies to minimize radar cross sections, and in antenna systems to enhance radiation efficiency and reduce mutual coupling. Moreover, its polarization insensitive characteristics make it promising for use in satellite communication, radar sensing, and 5G/6G wireless systems

operating within the Ku/Ka frequency bands.

AI Contribution Statement:

Artificial intelligence tool (ChatGPT by OpenAI) were used only for language refinement and grammar editing.

REFERENCES

Pendry, J. B., Schurig, D., & Smith, D. R. (2006). Controlling electromagnetic fields. *science*, *312*(5781), 1780-1782. https://doi.org/10.1126/science.1125907

Singh, H., Mittal, N., Gupta, A., Kumar, Y., Woźniak, M., & Waheed, A. (2021). Metamaterial integrated folded dipole antenna with low SAR for 4G, 5G and NB-IoT applications. *Electronics*, *10*(21), 2612. https://doi.org/10.3390/electronics10212612

Smith, D. R., Pendry, J. B., & Wiltshire, M. C. (2004). Metamaterials and negative refractive index. *science*, *305*(5685), 788-792. https://doi.org/10.1126/science.1096796

Kıymaz, Y. E., & Oguz, H. (2024). Assessment of electricity generation using deep learning on solar power plants. *Necmettin Erbakan Üniversitesi Fen ve Mühendislik Bilimleri Dergisi*, *6*(2), 289-311. https://doi.org/10.47112/neufmbd.2024.49

Akkoyunlu, M. T., Polat, E., Özkılıçaslan, R., Keleş, V., Abdallatif, Y., & Samancı, A. (2024). Güneş enerji santralinin temizlik sonrası üretim verilerinin incelenmesi. *Necmettin Erbakan Üniversitesi Fen ve Mühendislik Bilimleri Dergisi*, *6*(3), 583-591. https://doi.org/10.47112/neufmbd.2024.67

Ateş, T. F., Açıkgöz, H., & Özkan, A. O. (2019). Pasif RFID Etiket konumunu belirlemeye yönelik UHF anten tasarımı. *Necmettin Erbakan Üniversitesi Fen ve Mühendislik Bilimleri Dergisi*, *1*(2), 112-117.

Engheta, N. (2002, June). Thin absorbing screens using metamaterial surfaces. In *IEEE Antennas and Propagation Society International Symposium (IEEE Cat. No. 02CH37313)* (Vol. 2, pp. 392-395). IEEE. https://doi.org/10.1109/APS.2002.1016106

Watts, C. M., Liu, X., & Padilla, W. J. (2012). Metamaterial electromagnetic wave absorbers. *Advanced materials*, *24*(23), OP98-OP120. https://doi.org/10.1002/adma.201200674

Ünal, E., Dincer, F., Tetik, E., Karaaslan, M., Bakir, M., & Sabah, C. (2015). Tunable perfect metamaterial absorber design using the golden ratio and energy harvesting and sensor applications. *Journal of Materials Science: Materials in Electronics*, *26*(12), 9735-9740. https://doi.org/10.1007/s10854-015-3642-7

Nowak, M. (2021). Metamaterial-based sub-microwave electromagnetic field energy harvesting system. *Energies*, *14*(12), 3370. https://doi.org/10.3390/en14123370

Bağmancı, M., Karaaslan, M., Ünal, E., Akgol, O., Karadağ, F., & Sabah, C. (2017). Broad-band polarization-independent metamaterial absorber for solar energy harvesting applications. *Physica E: low-dimensional systems and nanostructures*, *90*, 1-6. https://doi.org/10.1016/j.physe.2017.03.001

Liu, H., Xie, M., Ai, Q., & Yu, Z. (2021). Ultra-broadband selective absorber for near-perfect harvesting of solar energy. *Journal of Quantitative Spectroscopy and Radiative Transfer*, *266*, 107575. https://doi.org/10.1016/j.jqsrt.2021.107575

Khanna, Y., & Awasthi, Y. K. (2020, February). Wideband Ultra-thin Metamaterial Absorber for Ku & K-Band Applications. In *2020 7th International Conference on Signal Processing and Integrated Networks (SPIN)* (pp. 367-371). IEEE. https://doi.org/10.1109/SPIN48934.2020.9070938

Bilal, R. M. H., Baqir, M. A., Choudhury, P. K., Karaaslan, M., Ali, M. M., Altınntas, O., ... & Sabah, C. (2021). Wideband microwave absorber comprising metallic split-ring resonators surrounded with E-shaped fractal metamaterial. *IEEE Access*, *9*, 5670-5677. https://doi.org/10.1109/ACCESS.2020.3048927

Chung, M., Jeong, H., Kim, Y. K., Lim, S., & Baek, C. W. (2022). Design and fabrication of millimeter-wave frequency-tunable metamaterial absorber using MEMS cantilever actuators. *Micromachines*, *13*(8), 1354. https://doi.org/10.3390/mi13081354

Hakim, M. L., Alam, T., Islam, M. T., Alsaif, H., & Soliman, M. S. (2023). Polarization-independent fractal square splits ring resonator (FSSRR) multiband metamaterial absorber/artificial magnetic conductor/sensor for Ku/K/Ka/5G (mm-Wave) band applications. *Measurement*, *210*, 112545. https://doi.org/10.1016/j.measurement.2023.112545

Zhu, J. F., Sheng, Y. W., Gao, G. L., Shi, M. C., Ruan, J. F., Deng, G. S., & Yin, Z. P. (2025). Ultrathin and flexible broadband metamaterial absorber for Ka-band applications. *Optical Materials Express*, *15*(2), 152-163. https://doi.org/10.1364/OME.547974

Zhong, M., Jiang, X., Zhu, X., Zhang, J., & Zhong, J. (2020). Design and fabrication of a single metal layer tunable metamaterial absorber in THz range. *Optics & Laser Technology*, *125*, 106023. https://doi.org/10.1016/j.optlastec.2019.106023

Nickpay, M. R., Danaie, M., & Shahzadi, A. (2021). A wideband and polarization-insensitive graphene-based metamaterial absorber. *Superlattices and Microstructures*, *150*, 106786. https://doi.org/10.1016/j.spmi.2020.106786

Hanif, A., Hakim, M. L., Alam, T., Islam, M. T., Alsaif, H., & Soliman, M. S. (2023). Polarization insensitive oblique incident angle stable ultra-thin nano ring resonator-based metamaterial absorber for visible and near-infrared region applications. *Optics & Laser Technology*, *164*, 109494. https://doi.org/10.1016/j.optlastec.2023.109494

Dincer, F., Karaaslan, M., Unal, E., & Sabah, C. (2013). Dual-band polarization independent metamaterial absorber based on omega resoanator and octa-star strip configuration. *Progress In Electromagnetics Research*, *141*, 219-231. http://dx.doi.org/10.2528/PIER13061105

Ünal, E., Bağmancı, M., Karaaslan, M., Akgol, O., Arat, H. T., & Sabah, C. (2017). Zinc oxide–tungsten-based pyramids in construction of ultra-broadband metamaterial absorber for solar energy harvesting. *IET Optoelectronics*, *11*(3), 114-120. https://doi.org/10.1049/iet-opt.2016.0138

Guo, Z., Liu, X., Li, C., Li, J., Cai, H., Fu, M., ... & Wang, Y. (2021). Near-perfect broadband metamaterial absorbers of truncated nanocones using colloidal lithography. *Optical Materials*, *119*, 111352. https://doi.org/10.1016/j.optmat.2021.111352

Ning, J., Chen, K., Zhao, W., Zhao, J., Jiang, T., & Feng, Y. (2022). An ultrathin tunable metamaterial absorber for lower microwave band based on magnetic nanomaterial. *Nanomaterials*, *12*(13), 2135. https://doi.org/10.3390/nano12132135

Saadeldin, A. S., Sayed, A. M., Amr, A. M., Sayed, M. O., Hameed, M. F. O., & Obayya, S. S. A. (2023a). Broadband polarization insensitive metamaterial absorber. *Optical and Quantum Electronics*, *55*(7), 652. https://doi.org/10.1007/s11082-023-04881-y

Saadeldin, A. S., Sayed, A. M., Amr, A. M., Sayed, M. O., Hameed, M. F. O., & Obayya, S. S. A. (2023b). Wideband ultrathin and polarization insensitive metamaterial absorber for Ku-band applications. *Journal of Materials Science: Materials in Electronics*, *34*(26), 1797. https://doi.org/10.1007/s10854-023-11157-4

Uddin, M. K., Islam, M. T., Alam, T., Sahar, N. M., Alsaif, H., Hakim, M. L., & Islam, M. R. (2025). Polarization insensitive U-coupled splits ring resonator-based hexa-band metamaterial absorber for concentration of solid material sensing applications. *Optics & Laser Technology*, *181*, 111975. https://doi.org/10.1016/j.optlastec.2024.111975

Landy, N. I., Sajuyigbe, S., Mock, J. J., Smith, D. R., & Padilla, W. J. (2008). Perfect metamaterial absorber. *Physical review letters*, *100*(20), 207402. https://doi.org/10.1103/PhysRevLett.100.207402

Cai, W., & Shalaev, V. M. (2016). *Optical metamaterials: fundamentals and applications* (Vol. 2, No. 1). New York: springer. https://doi.org/10.1007/978-1-4419-1151-3

Balanis, C. A. (2016). *Antenna theory: analysis and design*. John wiley & sons.

Ibrahım, M. A. (2025). *Ku ve Ka-Bant Uygulamaları İçin Geniş Bantlı Ultra Ince ve Polarizasyona Duyarlı Olmayan Metamalzeme Soğurucu* (Master's thesis, Necmettin Erbakan University (Turkey)).